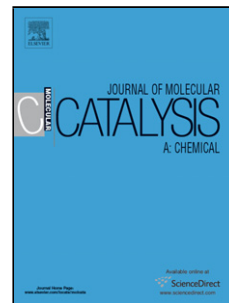


Accepted Manuscript

Title: Production of nanocatalyst from natural magnetite by glow discharge plasma for enhanced catalytic ozonation of an oxazine dye in aqueous solution

Author: Mojtaba Taseidifar Alireza Khataee Behrouz Vahid
Sirous Khorram Sang Woo Joo



PII: S1381-1169(15)00177-6
DOI: <http://dx.doi.org/doi:10.1016/j.molcata.2015.05.004>
Reference: MOLCAA 9490

To appear in: *Journal of Molecular Catalysis A: Chemical*

Received date: 25-12-2014
Revised date: 4-5-2015
Accepted date: 5-5-2015

Please cite this article as: Mojtaba Taseidifar, Alireza Khataee, Behrouz Vahid, Sirous Khorram, Sang Woo Joo, Production of nanocatalyst from natural magnetite by glow discharge plasma for enhanced catalytic ozonation of an oxazine dye in aqueous solution, *Journal of Molecular Catalysis A: Chemical* <http://dx.doi.org/10.1016/j.molcata.2015.05.004>

This is a PDF file of an unedited manuscript that has been accepted for publication. As a service to our customers we are providing this early version of the manuscript. The manuscript will undergo copyediting, typesetting, and review of the resulting proof before it is published in its final form. Please note that during the production process errors may be discovered which could affect the content, and all legal disclaimers that apply to the journal pertain.

Production of nanocatalyst from natural magnetite by glow discharge plasma for enhanced catalytic ozonation of an oxazine dye in aqueous solution

Mojtaba Taseidifar^a, Alireza Khataee^{a*} a_khataee@tabrizu.ac.ir or khataee@yahoo.com,

Behrouz Vahid^b, Sirous Khorram^c, Sang Woo Joo^{d**} swjoo@yu.ac.kr

^aResearch Laboratory of Advanced Water and Wastewater Treatment Processes, Department of Applied Chemistry, Faculty of Chemistry, University of Tabriz, 51666-16471 Tabriz, Iran

^bDepartment of Chemical Engineering, Tabriz Branch, Islamic Azad University, 51579-44533 Tabriz, Iran

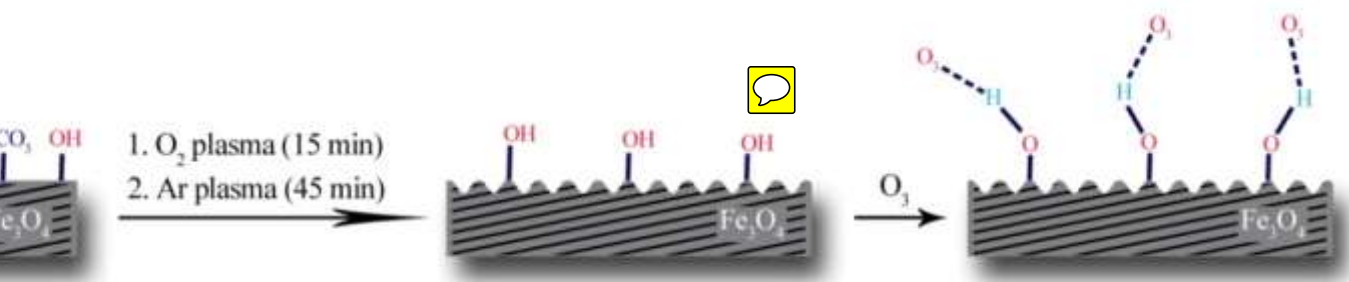
^cResearch Institute for Applied Physics and Astronomy, University of Tabriz, 51666-16471 Tabriz, Iran

^dSchool of Mechanical Engineering, Yeungnam University, 712-749 Gyeongsan, South Korea

*Corresponding author. Tel.: +98 41 33393165; Fax: +98 41 33340191

** Corresponding author: Tel: +82 53 810 1456

Graphical abstract



Proposed model for the interaction of glow discharge (O₂-Ar) plasma and

O₃ with catalyst surface.

Highlights

- Modification of natural magnetite by oxygen and argon glow discharge plasma.
- Characterization of the plasma treated magnetite by XRD, FT-IR, SEM, BET and pH_{PZC} .
- Application of plasma treated magnetite in heterogeneous catalytic ozonation process.
- Evaluation of effective parameters on heterogeneous ozonation process.

Abstract

Cheap natural magnetite (NM) was modified with oxygen plasma owing to its cleaning effect by chemical etching and with argon plasma due to its sputtering effect resulting in more surface roughness. These plasmas were utilized individually or in the order of first O₂ and then Ar plasmas, respectively. The performance of the plasma treated magnetites (PTMs) was higher than NM for treatment of Basic Blue 3 (BB3) in catalytic ozonation (O₃/PTM). The properties of NM and the most efficient treated magnetite (PTM₄) samples were characterized by X-ray diffraction (XRD), Fourier transform infrared spectroscopy (FT-IR), Brunauer-Emmett-Teller (BET) and scanning electron microscopy (SEM) methods. The optimal values were chosen for operational parameters including ozone concentration (0.3 g/L), initial pH (6.7) and PTM₄ dosage (600 mg/L). GC-Mass analysis was applied to detect intermediates. Environmentally-friendly treatment of the NM, simple separation of the catalyst, negligible leached iron concentration, successive reusability at milder pH and unaffected efficiency in the presence of inorganic salts are the main advantages of the PTM₄.

Keywords

Nanocatalyst; Magnetite nanoparticles; Catalytic ozonation; Oxygen glow discharge; Argon glow discharge.

1. Introduction

Wastewater of textile industries have extensive amounts of various dyes, which are commonly bio-resistant and as a consequence conventional biological methods are not efficient for their remediation [1]. Moreover, other physico-chemical processes like adsorption and coagulation merely transfer pollutants to secondary phases, that need more treatment [2]. Hence, applications of advanced oxidation processes (AOPs) are more proper not only for degradation, but also for mineralization of diverse contaminants with no extra waste [3]. Among reactive oxygen species (ROS), hydroxyl radicals ($\cdot\text{OH}$) have the significant role in AOPs due to unselective reaction with organic pollutants and their conversion to harmless compounds like carbon dioxide, water and inorganic mineral salts [4]. Ozonation treatment is one of the effective AOPs applied for the removal of persistent organic pollutants (POPs) due to its high reactivity and disinfection ability [4, 5]. Degradation of POPs can be explained by decomposition of O_3 to generate $\cdot\text{OH}$ radicals in basic mediums (Eqs. 1 and 2) or by its direct electrophilic attack in acidic conditions [6]. However, it has been known that the appropriate degradation of pollutants may be not achieved by O_3 alone process [7].



Heterogeneous catalyzed ozonation, which can be performed under ambient conditions is more efficient process for the removal of organic pollutants like humic and oxalic acids [8]. It can be attributed to more ozone dissolution and decomposition in the presence of solid particles due to ozone reaction with hydroxyl groups, which is existed on the surface of particles [9].

Stable form and abundance of magnetite (Fe_3O_4) makes it adequate for usage in the catalytic ozonation [10]. Furthermore, applications of nano-sized catalysts in heterogeneous ozonation results in more reaction sites and better mass transfer [8, 11]. However, different synthesis methods for producing nano-sized magnetite require toxic and expensive reactants [10].

Plasma is ionized gas that it comprises from positive and negative ions, electrons and neutral species, which is considered as the fourth state of matter, solves the above-mentioned problems by an environmentally-friendly method [12]. Recently, non-thermal plasma methods including glow discharge, silent discharge, and radio frequency discharge have been applied for surface modification of various catalysts and improvement of their performance [13, 14]. For instance, the plasma treatment changes the surface structure and activity of synthesized zeolites or natural clinoptilolite [13]. Besides, stability and catalytic activity of the Pd/HZSM-5 catalyst enhance after treatment by plasma [15]. In addition, plasma-modified $\text{Fe}_2\text{O}_3/\text{ZSM-5}$ catalyst with the high activity and selectivity for hydrogenation of carbon monoxide is obtained using the glow discharge of oxygen and argon [16].

To the best of our knowledge, there have been no reports regarding to the surface modification of natural magnetite particles under the glow discharge plasma for using in water treatment process. So, in this study first, a novel method to generate nanostructured magnetite utilizing the plasma method is presented. The characterizations of treated NM were performed by X-ray diffraction (XRD), Fourier transform infrared spectroscopy (FT-IR), Brunauer-Emmett-Teller (BET) and scanning electron microscopy (SEM) methods. Then, the efficiency of PTM in heterogeneous catalytic ozonation for the decolorization of BB3 was evaluated and compared with NM. Finally, the effect of operational parameters include dye concentration, ozone concentration, initial pH, organic, PTM dosage and additional of inorganic salts were carried out and some of the generated intermediates during the process were identified by GC-Mass.

2. Experimental

2.1. Materials

Natural magnetite was provided from Sarab, Iran, which was very cheap and abundant. Elemental composition of NM was identified (O, 52.85%; Fe, 10.54%; C, 21.18%; Si, 14.25% and Ti, 1.18%) by X-ray photoelectron spectroscopy (XPS) using K-ALPHA Thermo Scientific spectrometer (UK). C.I. BB3 (color index number: 45170, molecular formula = $C_{20}H_{26}N_3OCl$, $\lambda_{max} = 654$ nm and $M_w = 359.89$ g/mol), which is a cationic mono-oxazine dye, purchased from Boyakhsaz Co., Iran. Its chemical structure is shown in Fig. 1.

BB3 is used extensively for dyeing of wool and acrylic fibers with lethal dose 50 (LD_{50}) of 100 mg/kg for rats [17]. All of the other chemicals were of analytical grade and they were provided from Merck, Germany.

2.2. Procedure of catalyst treatment and characterization methods

NM sample was crushed to prepare particles with diameter between 210 and 354 μm and the obtained particles were washed with distilled water and they dried at 60-70 $^{\circ}C$ for 24 h. Then, non-thermal plasma technique was used for rejuvenation of them (3 g) using a plasma reactor made up of a Pyrex tube equipped with two electrodes on its sides (Fig. 2).

DC high-voltage (1200 V) was applied on electrodes to generate glow discharge plasma. Oxygen and/or argon at a flow of 3 standard cubic centimeters per second were fed to the

plasma reactor individually to generate the plasma. Table 1 presents the type and applied time of the mentioned gases in the plasma reactor.

After the modifying process, the PTM particles were collected for using in heterogeneous ozonation. In order to characterization of NM and the most effective plasma treated magnetite (PTM₄), the following analyses were performed: 1) the phase identification was carried out by X-ray diffraction (XRD) technique (PANalytical X'Pert PRO, Germany) with Cu- α radiation (45 kV, 40 mA, 0.15406 nm). 2) Fourier transform infrared (FT-IR) spectra of the samples were obtained by Tensor 27, Bruker spectrometer (Germany). 3) Scanning electron microscopy (S-4200 Hitachi, Japan) was applied to identify their morphology and dimensions. 4) The porosity of the samples was evaluated by physical adsorption of N₂ at 77 K using Nitrometrics Gmini series (Japan). 5) the pH of point of zero charge (pH_{PZC}) was determined according to the salt addition method [18].

2.3. Catalytic ozonation set-up and procedure

The ozonation set-up was illustrated in Fig. 3.

Experiments were carried out in batch mode by a cylindrical reactor (Pyrex, 36 cm height \times 4.5 cm internal diameter). To generate ozone, oxygen gas, which was provided by oxygen generator (Airsep, USA), was fed into the laboratory ozone generator (Donali, Iran). Then, the ozone was continuously fed into the solution through a diffuser at the bottom of the reactor and its concentration was adjusted by changing the gas flow (1 to 5 L/min) with ozone-dissolved concentration between 0.3 and 2.5 mg/L and determined by indigo trisulfonate method according to the procedure proposed by Bader and Hoigne [19]. In each

experiment, 250 mL of the reaction mixture contained definite concentration of BB3 and catalyst (NM or PTM) was prepared. Sulfuric acid and sodium hydroxide were used for pH adjustment of the solution. Then, the solution was treated by chosen O₃ dosage. At distinct process time-intervals, samples were withdrawn by a glass syringe, and then the magnetic catalyst particles were separated from the solution by an external magnet. Eventually, the sample was analyzed for degradation amount of BB3 concentration by UV-Vis spectrophotometer (WPA Lightwave S2000, England) at 654 nm. In order to identify the BB3 degradation intermediates during O₃/PTM process, GC-Mass analysis was performed using an Agilent 6890 gas chromatograph with a 30 m–0.25 mm HP-5MS capillary column coupled with an Agilent 5973 mass spectrometer (Agilent Technologies, Palo Alto, Canada) [20]. Influence of inorganic salts including sodium chloride (1 mM) and sodium sulfate (1 mM) were applied as hydroxyl radical scavengers [4]; the dissolved iron concentration was measured colorimetrically with 1,10-phenanthroline at 510 nm by UV-Vis spectrophotometer in O₃/PTM₄ process [21].

3. Results and discussion

3.1. Comparison of various treatment processes for degradation of BB3 and kinetics study

The ozonation and catalytic ozonation processes for the degradation of a model contaminant (BB3) in aqueous solution were compared using NM and various plasma treated samples. The adsorptions of dye by all the samples were negligible and obtained less than 7% in optimal condition after 20 min. All of the applied AOPs in this study followed pseudo-first order kinetic, which is in consistent with other similar studies [22, 23].

In the depicted plots of $\ln(A_0/A)$ against time (t), straight lines with high correlation coefficients (R^2), which was more than 0.96, confirmed the suggested first order kinetic.

Then, from the slope of plots, the apparent pseudo-first order rate constants (k_{app}) for the degradation of BB3 were determined and presented in Table 1. As can be seen from Fig. 4, the degradation efficiency of BB3 after 15 min of treatment at the same operational conditions was obtained as 51.02, 63.78 and 93.47% for O_3 , O_3/NM and O_3/PTM_4 (the most efficient plasma surface modified catalyst) processes. Hence, PTM_4 was selected as the desired catalyst for identification of this structure and further experiments in catalytic ozonation.

3.2. Characterization of NM and PTM_4

The XRD patterns of the NM and PTM_4 samples are demonstrated in Fig. 5.

There are the same diffraction peaks at 2θ of 30.1, 35.5, 43.2, 53.5, 57.0 and 62.8 attributed to (2 2 0), (3 1 1), (4 0 0), (4 2 2), (5 1 1) and (4 4 0) panels of magnetite (Fe_3O_4 phase), respectively [24, 25]. Thus, these results demonstrate that the plasma treatment have no effect on the crystal structure of the NM.

Plasma treatment caused to decrease in the absorption peaks at 400 to 4000 cm^{-1} in FT-IR spectrum (Fig. 6), generally.

The peaks at 576 and 470 cm^{-1} correspond to Fe–O vibration [26, 27]. Moreover, the peak at 1641 cm^{-1} is attributed to C=O stretching vibration in carbonyl groups, which is almost vanished in PTM_4 . Besides, two peaks at about 2924 and 2853 cm^{-1} are assigned to asymmetric and symmetric C–H bonds, respectively [28]. The peak at 3450 cm^{-1} can be

attributed to O–H bond vibration [29]. Finally, the peak at 1046 cm^{-1} belongs to asymmetric O–Si–O stretching vibration bond [13].

SEM images of NM and PTM₄ samples with different magnifications are shown in Fig. 7.

Fig. 7 (a, b) demonstrates a bulk structure of the raw magnetite sample. SEM images of NM after 15 min of treatment by O₂ plasma were shown in Fig. 7 (c, d), which shows no considerable changes on the surface of NM. Comparison of the mentioned SEM images with Fig 7 (e, f) indicates nano-sized magnetite is formed on the surface of NM by Ar plasma-treated process after 45 min, which shows nano-structure of the catalyst surface. Specific surface area of the NM and PTM₄ were determined as 7.65 and 11.03 m²/g, respectively. Also, pH_{PZC} of the NM and PTM₄ were measured as 7.5 and 6.2, respectively.

3.3. Effect of plasma on the NM

The PTM₄ was produced from the NM utilizing O₂ plasma for 15 min, and then Ar plasma for 45 min. In the first step of the plasma treatment, as can be seen from SEM images (Fig. 7 (c, d)), the surface of the catalyst is not changed remarkably, which indicates the pure chemical etching resulting in formation of some gaseous products like CO₂ and H₂O [14, 30]. Besides, the O₂ plasma can remove the carbon from the catalyst surface and cause to better performance by regenerating of active sites [31]. Furthermore, O₃ can be generated during the utilization of O₂ plasma [32], which can decline in the bands related to the surface hydroxyl and carbonate groups. However, after treatment by O₃ and scavenging of the mentioned species, some of the hydroxyl groups remain on the surface of the catalyst [33], which can interact with ozone in solution in O₃/PTM₄ process. The decrease in FT-IR peaks in the sample after plasma treatment confirms the mentioned mechanism, as can be observed CO band (1641 cm^{-1}) is disappeared almost completely but OH groups (3450 cm^{-1}) still remained

on the catalyst surface. This chemical cleaning effect of the surface by retaining of hydroxyl groups is the main reason of the better performance of the catalyst in the O_3/PTM process in comparison with O_3/NM . In the second step of the plasma treatment by applying of the high energy species generated by the Ar plasma, the surface of the catalyst was sputtered effectively by the positive ions from the argon plasma resulting in more surface roughness with nano-sized structure and increase in active sites of catalyst [34, 35]. Furthermore, the rate of ozone decomposition is strongly dependent on the specific surface area [36]. In the light of these facts outlined above, PTM_4 has better performance in catalytic ozonation than PTM_3 because it was modified with Ar gas more than O_2 gas. As can clearly be seen from SEM images (Fig. 7 (e, f)). Enhancement of the specific surface area of the catalyst from 7.65 (NM) to 11.03 m^2/g (PTM_4) after plasma treatment verifies the above-mentioned explanations and is the major reason for the more activity of the catalyst in the O_3/PTM_4 process compared to O_3/NM (Fig. 4).

3.4. Effect of operational parameters on the catalytic ozonation

The effect of main operational parameters including initial BB3 and ozone concentrations, pH, and catalyst (PTM_4) dosage on the degradation of the organic contaminant was studied. Effect of these parameters on the apparent pseudo-first order constant of degradation and mineralization for O_3/PTM_4 process was illustrated in Table 2.

Amount of operational parameters except for the above-mentioned ones: $[BB3]_0 = 600$ mg/L, pH = 6.7, O_3 concentration = 0.3 mg/L and PTM_4 dosage = 600 mg/L

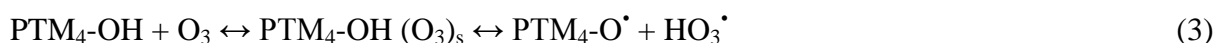
The degradation of BB3 was declined by increasing of its initial concentration (Fig. 8) because the identical amounts of produced oxidizing species at the same operational conditions had to degrade more BB3 and its degradation intermediates [37, 38].

As the applied ozone concentration was increased, the degradation of BB3 was enhanced due to the production of more ROS, particularly hydroxyl radicals [39]. In addition, a high ozone flow rate leads to the enhancement of the ozone mass transfer rate from gas phase to liquid phase [40]. By considering the high reactivity of the ozone and approximately the same obtained degradation efficiency of BB3 after 21 min, the flow rate of 1 L/h correspondent to 0.3 mg/L was chosen for performing of the other experiments. The degradation of BB3 was seemed to be efficient by the indirect attack of hydroxyl radicals in the more basic medium than the direct electrophilic attack in the acidic medium under the identical operational conditions (Fig. 9) [36, 39]; Moreover, the pH_{pzc} of the PTM_4 was measured as 6.2. At $\text{pH} > \text{pH}_{\text{pzc}}$, the surface of the catalyst has negative charge, which can adsorb the positive charge dye better than in $\text{pH} < \text{pH}_{\text{pzc}}$, due to the electrostatic repulsion effects.

However, the obtained results for pH of 6.7 (natural pH of the dye) and 9 did not differ considerably, hence pH of 6.7 was chosen as the optimum one. In addition, PTM_4 has the lower pH_{pzc} ($\text{pH}_{\text{pzc}}=6.2$) compared to NM ($\text{pH}_{\text{pzc}}=7.5$), which can adsorb the positive charged dye more effectively in the lower pHs, Hence, the better performance of the PTM_4 was observed in pH of 6.7 (Fig. 10).

Fig. 11 illustrates the interaction of O₃ with the hydroxyl groups on the catalyst surface after plasma treatment, which causes to generation of active radicals specially hydroxyl radicals to degrade the contaminant [33, 36]:

The hydroxyl groups existed on magnetite surface can catalyze the O₃ in solid phase and make a series of chain reactions (Fig. 11). The initial step involves the formation of a surface complex between ozone and the magnetite surface [6, 41], thus proposed mechanism for ozone decomposition on PTM₄ surface can be described as Eqs. 3-6. Similar study has been conducted by Park et al [41].



This phenomenon can be explained by the fact that with increasing PTM₄ dosage, the number of catalytic active sites is enhanced and accordingly more ozone molecules on the catalyst surface are decomposed to $^\bullet\text{OH}$ [41]. However no noticeable difference in degradation efficiency between 600 and 800 mg/L of the catalyst dosage was observed (Fig. 12). Therefore, 600 mg/L was selected as the desired dosage of the PTM₄.

3.5. Spectral changes of BB3 during the catalytic ozonation and reusability of the catalyst

The changes in UV-Vis absorption spectra of BB3 during PTM catalytic ozonation are shown in Fig. 13.

The decrease of absorption peak of BB3 at 654 nm indicated a rapid degradation of the dye and its complete degradation was achieved after 21 min at the desired experimental conditions. Furthermore, the absorption peak around 254 nm, gradually weakened and removed after 21 min of the treatment, without observing a new peak, which is related to the elimination of the aromatic rings [42].

The potential of the catalyst in successive application for removal of organic contaminants is significant from a practical point of view. Thus, three repetitive cycles for the degradation of BB3 were conducted (Fig. 14).

The applied catalyst was recovered by the magnetic separation and dried for the next degradation cycle. The PTM₄ exhibited the same activity as that obtained from the first run, which demonstrated not only the stability and reusability of the catalyst, but also the reliability of the results.

3.6. Effect of inorganic salts and dissolved iron concentration

The influence of inorganic anions such as sulfate (SO_4^{2-}) and chloride (Cl^-), which can be existed in textile effluents and acted as hydroxyl radical scavengers, was determined in O_3/PTM_4 . Catalytic ozonation process is just negligibly affected by the mentioned inorganic salts (Fig. 15), which is in consistent with the other study for degradation of mesoxalic and oxalic acids by catalytic ozonation [4].

The iron amount in the solution was measured colorimetrically based on Beer-Lambert law (Fig. 16).

After 30 min of treatment under optimal conditions the total iron amount was determined as 0.2 mg/L, which was lower than maximum concentration level of iron in drinking water (0.3 mg/L) [43]. Iron ions can catalyze O_3 resulting in production of $\cdot OH$ by the process of homogenous catalytic ozonation. Firstly, this reaction gives the Ferryl intermediate (FeO^{2+}), which could also generate hydroxyl radical (Eqs. 7 and 8) [44, 45].



3.7. Identification of intermediates in the catalytic ozonation process

In order to recognize the intermediates of BB3 degradation in the O_3/PTM_4 process, the dye solution was treated for 4 min under the optimal conditions and six produced intermediates were identified by comparison with commercial standards when the match factor of mass spectrum was above 90% (Table 3). Degradation of the dye can take place by cleavage of C-C or C-N bonds [46]. After opening the aromatic rings, short chained compounds like acids were formed, which could be converted directly to CO_2 for complete mineralization. Moreover, formation of compounds 3 and 4 considered to be related to interaction of unknown byproducts with each other quickly [47]. However, several chromatographic peaks could not be identified owing to their low match factor. In addition, some of the intermediates could not be recognized due to their rapid oxidization.

4. Conclusions

In this research, improvement of the natural magnetite activity by the low-temperature plasma treatment in the catalytic ozonation process for degradation of the oxazine dye can be attributed to the chemical cleaning and sputtering effects of O₂ and Ar plasmas, respectively. The most efficient modified catalyst (PTM₄) was prepared by utilizing O₂ and then Ar plasmas for 15 and 45 min, respectively. The obtained results were confirmed by decreasing of the absorption peaks in FT-IR spectra and the enhancement of surface area of PTM₄ compared to the NM. SEM images demonstrated the formation of nano-structured magnetite on the catalyst surface after plasma treatment. Based on the XRD patterns, the crystal structure of magnetite was not altered after plasma treatment. The effect of experimental parameters was investigated on the degradation efficiency of BB3 in O₃/PTM₄ process. Decolorization efficiency was declined by increasing of the pollutant concentration and enhanced by increasing of ozone concentration, PTM₄ dosage and pH. The proposed plasma treatment method for modification of the NM catalyst as a cheap and abundant material was environmentally friendly without using toxic chemicals for its synthesis. The PTM₄ can be effectively used in the repeated runs with simple separation by the external magnetic field. Moreover, it can be utilized in the milder pH medium and the inorganic salts have almost insignificant effect on the process.

Acknowledgement

The authors thank the University of Tabriz (Iran) for all of the support provided.

References

- [1] A.R. Khataee, M. Zarei, *Desalination*, 273 (2011) 453-460.
- [2] K. Rusevova, F.D. Kopinke, A. Georgi, *J. Hazard. Mater.*, 241-242 (2012) 433-440.
- [3] C.A. Orge, J.J.M. Orfao, M.F.R. Pereira, A.M. Duarte de Farias, M.A. Fraga, *Chem. Eng. J.*, 200-202 (2012) 499-505.
- [4] A.L. Petre, J.B. Carbajo, R. Rosal, E. Garcia-Calvo, J.A. Perdigon-Melon, *Chem. Eng. J.*, 225 (2013) 164-173.
- [5] A.R. Khataee, V. Vatanpour, A.R. Amani Ghadim, *J. Hazard. Mater.*, 161 (2009) 1225-1233.
- [6] B. Kasprzyk-Hordern, M. Ziołek, J. Nawrocki, *Appl. Catal. B, Environ.*, 46 (2003) 639-669.
- [7] Z. He, S. Song, M. Xia, J. Qiu, H. Ying, B. Lü, Y. Jiang, J. Chen, *Chemosphere*, 69 (2007) 191-199.
- [8] H. Zhao, Y. Dong, P. Jiang, G. Wang, J. Zhang, K. Li, *Cat. Sci. Tech.*, 4 (2014) 494-501.
- [9] S.-N. Zhu, K.N. Hui, X. Hong, K.S. Hui, *Chem. Eng. J.*, 242 (2014) 180-186.
- [10] H. Jung, J.-W. Kim, H. Choi, J.-H. Lee, H.-G. Hur, *Appl. Catal. B, Environ.*, 83 (2008) 208-213.
- [11] S. Zhang, X. Zhao, H. Niu, Y. Shi, Y. Cai, G. Jiang, *J. Hazard. Mater.*, 167 (2009) 560-566.
- [12] C.-j. Liu, J. Zou, K. Yu, D. Cheng, Y. Han, J. Zhan, C. Ratanatawanate, B.W.L. Jang, *Pure Appl. Chem.*, 78 (2006) 1227-1238.
- [13] A. Khataee, S. Bozorg, S. Khorram, M. Fathinia, Y. Hanifehpour, S.W. Joo, *Ind. Eng. Chem. Res.*, 52 (2013) 18225-18233.
- [14] P. Attri, B. Arora, E.H. Choi, *RSC Adv.*, 3 (2013) 12540-12567.

- [15] C.-j. Liu, K. Yu, Y.-p. Zhang, X. Zhu, F. He, B. Eliasson, *Appl. Catal. B, Environ.*, 47 (2004) 95-100.
- [16] E.A.Y. Dadashova, T. V.; Beilin, L. A.; Shpiro, E. S.; Lunin, V. V.; Kiselev, V.V.; , The regeneration of the Fe₂O₃ /Zeolite catalyst for Fischer-Tropsch synthesis in oxygen glow discharge, *Kinet. Catal. (Engl. Trans.)*, 1993.
- [17] R. Anliker, G. Durig, D. Steinle, E.J. Moriconi, *J. Soc. Dyers and Colourists*, 104 (1988) 223-225.
- [18] S. Mustafa, B. Dilara, K. Nargis, A. Naeem, P. Shahida, *Colloids and Surfaces A: Physicochem. Eng. Aspects*, 205 (2002) 273-282.
- [19] H. Bader, J. Hoigne, *Water Res.*, 15 (1981) 449-456.
- [20] B. Vahid, A. Khataee, *Electrochim. Acta*, 88 (2013) 614-620.
- [21] C. Adan, A. Bahamonde, I. Oller, S. Malato, A. Martinez-Arias, *Appl. Catal. B, Environ.*, 144 (2014) 269-276.
- [22] M.H. Priya, G. Madras, *Ind. Eng. Chem. Res.*, 45 (2006) 913-921.
- [23] T. Mousanejad, M. Khosravi, S.M. Tabatabaie, A.R. Khataee, K. Zare, *Res. Chem. Intermed.*, 40 (2014) 711-722.
- [24] H. Niu, D. Zhang, S. Zhang, X. Zhang, Z. Meng, Y. Cai, *J. Hazard. Mater.*, 190 (2011) 559-565.
- [25] Y. Leng, W. Guo, X. Shi, Y. Li, L. Xing, *Ind. Eng. Chem. Res.*, 52 (2013) 13607-13612.
- [26] A.M. Atta, O.E. El-Azabawy, H.S. Ismail, M.A. Hegazy, *Corros. Sci.*, 53 (2011) 1680-1689.
- [27] K.R. Reddy, W. Park, B.C. Sin, J. Noh, Y. Lee, *J. Colloid Interface Sci.*, 335 (2009) 34-39.
- [28] S. Aber, A. Khataee, M. Sheydaei, *Bioresour. Technol.*, 100 (2009) 6586-6591.
- [29] R. Chen, G. Song, Y. Wei, *J. Phys. Chem. C*, 114 (2010) 13409-13413.

- [30] H.L. Chen, H.M. Lee, S.H. Chen, M.B. Chang, S.J. Yu, S.N. Li, *Environ. Sci. Tech.*, 43 (2009) 2216-2227.
- [31] X. Yang, Y.C. Kimmel, J. Fu, B.E. Koel, J.G. Chen, *ACS Catal.*, 2 (2012) 765-769.
- [32] H.-H. Kim, A. Ogata, S. Futamura, *Appl. Catal. B, Environ.*, 79 (2008) 356-367.
- [33] M. Magureanu, D. Piroi, N.B. Mandache, V.I. Parvulescu, V. Parvulescu, B. Cojocaru, C. Cadigan, R. Richards, H. Daly, C. Hardacre, *Appl. Catal. B, Environ.*, 104 (2011) 84-90.
- [34] K.K. Ostrikov, I. Levchenko, U. Cvelbar, M. Sunkara, M. Mozetic, *Nanoscale*, 2 (2010) 2012-2027.
- [35] X. Zhu, P.-p. Huo, Y.-p. Zhang, C.-j. Liu, *Ind. Eng. Chem. Res.*, 45 (2006) 8604-8609.
- [36] H. Valdes, R.F. Tardon, C.A. Zaror, *Chem. Eng. J.*, 211-212 (2012) 388-395.
- [37] M. Sui, S. Xing, L. Sheng, S. Huang, H. Guo, *J. Hazard. Mater.*, 227-228 (2012) 227-236.
- [38] C.-C. Chang, C.-Y. Chiu, C.-Y. Chang, C.-F. Chang, Y.-H. Chen, D.-R. Ji, Y.-H. Yu, P.-C. Chiang, *J. Hazard. Mater.*, 161 (2009) 287-293.
- [39] A. Rodriguez, R. Rosal, J.A. Perdigon-Melon, M. Mezcua, A. Aguera, M.D. Hernando, P. Leton, A.R. Fernandez-Alba, E. Garcia-Calvo, *Ozone-Based Technologies in Water and Wastewater Treatment*, in, Springer Berlin Heidelberg, 2008,.
- [40] S. Song, J. Yao, Z. He, J. Qiu, J. Chen, *J. Hazard. Mater.*, 152 (2008) 204-210.
- [41] J.-S. Park, H. Choi, J. Cho, *Water Res.*, 38 (2004) 2285-2292.
- [42] M.A. Behnajady, N. Modirshahla, M. Mirzamohammady, B. Vahid, B. Behnajady, *J. Hazard. Mater.*, 160 (2008) 508-513.
- [43] S. Chaturvedi, P.N. Dave, *Desalination*, 303 (2012) 1-11.
- [44] C. Canton, S. Esplugas, J. Casado, *Appl. Catal. B, Environ.*, 43 (2003) 139-149.
- [45] L.F. Liotta, M. Gruttadauria, G. Di Carlo, G. Perrini, V. Librando, *J. Hazard. Mater.*, 162 (2009) 588-606.

[46] A.R. Khataee, M. Fathinia, S. Aber, M. Zarei, *J. Hazard. Mater.*, 181 (2010) 886-897.

[47] T. Hosoya, H. Kawamoto, S. Saka, *J. Anal. Appl. Pyrolysis*, 80 (2007) 118-125.

Figure caption

Fig. 1. Chemical structure of Basic Blue 3.

Fig. 2. Schematic diagram of the glow discharge plasma system.

Fig. 3. Schematic of experimental set-up of catalytic ozonation system.

Fig. 4. Comparison of O_3 , O_3/NM and O_3/PTM_4 ozonation in degradation of BB3. The inset shows mentioned processes follow pseudo-first order kinetic. Experimental conditions: catalyst dose: 600 mg/L, initial BB3 concentration: 90 mg/L, ozone concentration: 1.2 g/L and initial pH: 6.7.

Fig. 5. XRD patterns of NM and PTM_4 samples.

Fig. 6. FT-IR spectra of NM and PTM_4 samples.

Fig. 7. SEM images of NM (a, b), NM exposure to O_2 plasma (15 min) (c, d) and PTM_4 (e, f).

Fig. 8. Effect of initial BB3 concentration on the degradation of BB3 during PTM_4 catalytic ozonation. The inset shows mentioned processes follow pseudo-first order kinetic. Experimental conditions: PTM_4 dose: 600 mg/L, ozone concentration: 0.3 g/L and initial pH: 6.7.

Fig. 9. Effect of ozone concentration on the degradation of BB3 during PTM_4 catalytic ozonation. The inset shows mentioned processes follow pseudo-first order kinetic. Experimental conditions: PTM dose: 600 mg/L, initial BB3 concentration: 90 mg/L and initial pH: 6.7.

Fig. 10. Effect of initial pH on the PTM_4 catalytic ozonation of BB3. Experimental conditions: PTM dose: 600 mg/L, initial BB3 concentration: 90 mg/L and ozone concentration: 0.3 g/L.

Fig. 11. Proposed model for the interaction of glow discharge (O_2 -Ar) plasma and O_3 with catalyst surface.

Fig. 12. Effect of initial PTM₄ concentration on the catalytic ozonation of BB3. The inset shows mentioned processes follow pseudo-first order kinetics. Experimental conditions: initial BB3 concentration: 90 mg/L, ozone concentration: 0.3 g/L and initial pH: 6.7.

Fig. 13. Change in UV-Visible spectra of BB3 solution PTM₄ catalytic ozonation process at different times. Experimental conditions: catalyst dose: 600 mg/L, initial BB3 concentration: 90 mg/L, ozone concentration: 0.3 g/L and initial pH: 6.7.

Fig. 14. Reusability of PTM₄ on PTM₄ catalytic ozonation of BB3. Experimental conditions: PTM dose: 600 mg/L, initial BB3 concentration: 90 mg/L, ozone concentration: 0.3 g/L, and initial pH: 6.7.

Fig. 15. Effect of addition different salts on the degradation of BB3 during PTM₄ catalytic ozonation. Experimental conditions: PTM₄ dose: 600 mg/L, initial BB3 concentration: 90 mg/L, initial salts concentration: 1 mM, ozone concentration: 0.3 g/L, and initial pH: 6.7.

Fig. 16. Evolution of total iron leached from the PTM₄ catalyst. Experimental conditions: PTM dose: 600 mg/L, ozone concentration: 0.3 g/L and initial pH: 6.7.


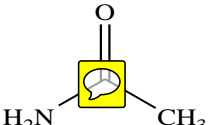

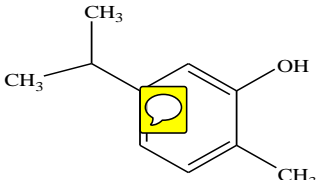
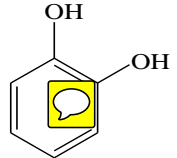
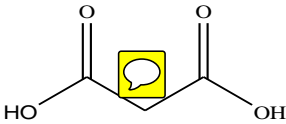
Table 1. Effect of the different catalytic ozonation and ozonation on the apparent pseudo-first-order constants of degradation and mineralization of BB3.

No.	Process	Type and time of applied gases in plasma	k_{app} (min^{-1})	R^2
1	O_3	–	0.0510	0.96
2	O_3/NM	–	0.0734	0.98
3	O_3/PTM_1	O_2 (60 min)	0.1295	0.99
4	O_3/PTM_2	Ar (60 min)	0.1685	0.98
5	O_3/PTM_3	O_2 (45 min) + Ar (15 min)	0.1384	0.97
6	O_3/PTM_4	O_2 (15 min) + Ar (45 min)	0.1814	0.97

Table 2. Effect of the operational parameters on the apparent pseudo-first order constant of degradation and mineralization for O₃/PTM₄ process.

Operational parameters and amounts	k _{app} (min ⁻¹)	Correlation coefficient (R ²)
BB3 concentration		
(mg/L)		
60	0.2175	0.99
90	0.1814	0.97
120	0.1370	0.96
150	0.1122	0.95
pH		
3	0.08	0.97
6.7	0.1814	0.97
9	0.26	0.94
O ₃ concentration (mg/L)		
0.3	0.1814	0.97
1.2	0.20	0.99
2.5	0.21	0.97
PTM ₄ dosage (mg/L)		
300	0.067	0.99
400	0.094	0.98
600	0.1814	0.97
800	0.202	0.99

Table 3. Identified by-products during catalytic ozonation of BB3 at 21 °C after 4 min of reaction at pH of 6.5 and ozone flow rate of 1 L/h.

No.	Compound	Structure	t _R (min)	Main fragments (m/z)/ (percent)
1 ^a	Acetic acid		4.581	75.00 (100.00%), 116.10 (76.7%), 73.10 (13.34%), 76.00 (7.52%), 117.00 (7.46%)
2 ^b	Ethanimidic acid		5.092	147.10 (100.00%), 73.10 (86.69%), 148.10 (42.73%), 203.10 (37.34%), 188.10 (22.50%)
3 ^b	Carbodiimide		5.292	171.10 (100.00%), 172.10 (16.28%), 173.00 (7.13%), 73.10 (7.12%), 78.00 (4.81%)
4 ^a	2-methyl-5-(1-methylethyl)phenol		12.438	207.00 (100.00%), 73.10 (30.28%), 222.10 (26.26%), 208.10 (18.17%), 209.10 (5.21%)
5 ^a	Benzene-1,2-diol		6.812	28.10 (100.00%), 151.00 (56.89%), 75.00 (31.69%), 32.00 (25.97%), 166.10 (16.69%)
6 ^a	Propanedioic acid		12.014	147.10 (100.00%), 73.00 (67.79%), 305.20 (42.42%), 189.10 (33.03%), 75.00 (19.44%)

^a Value corresponding to the trimethylsilyl derivative

^b Value corresponding to the bis trimethylsilyl derivative

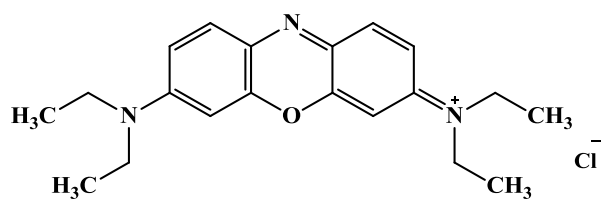


Fig. 1. Chemical structure of Basic Blue 3.

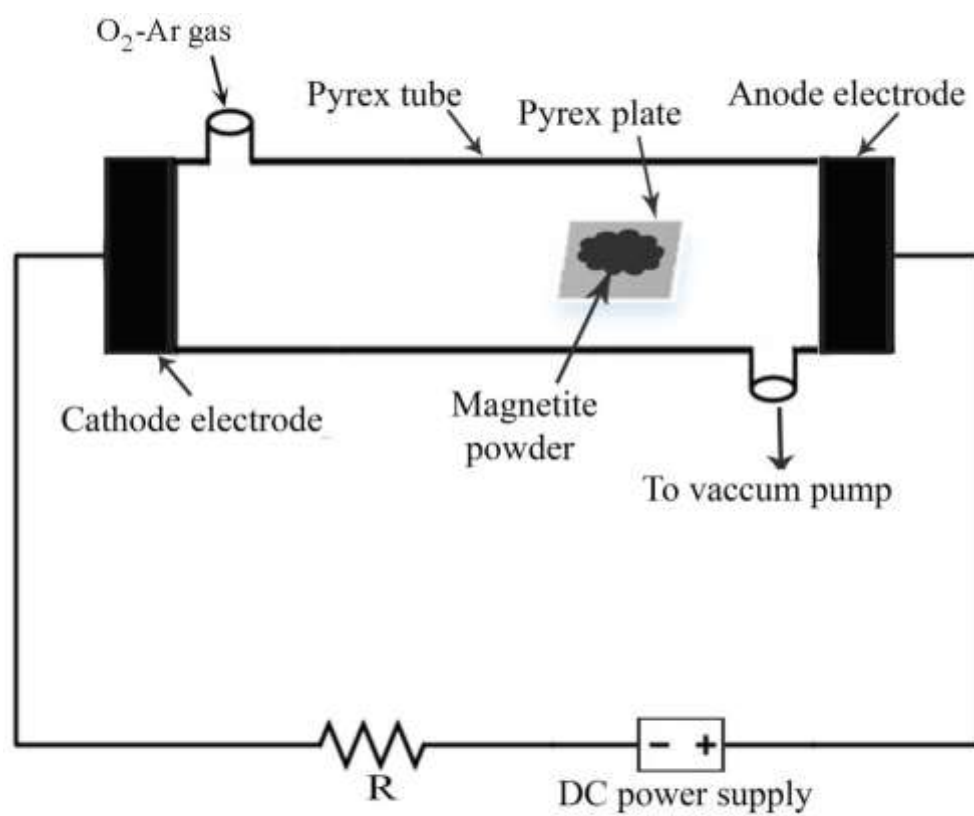


Fig 2. Schematic diagram of the glow discharge plasma system.

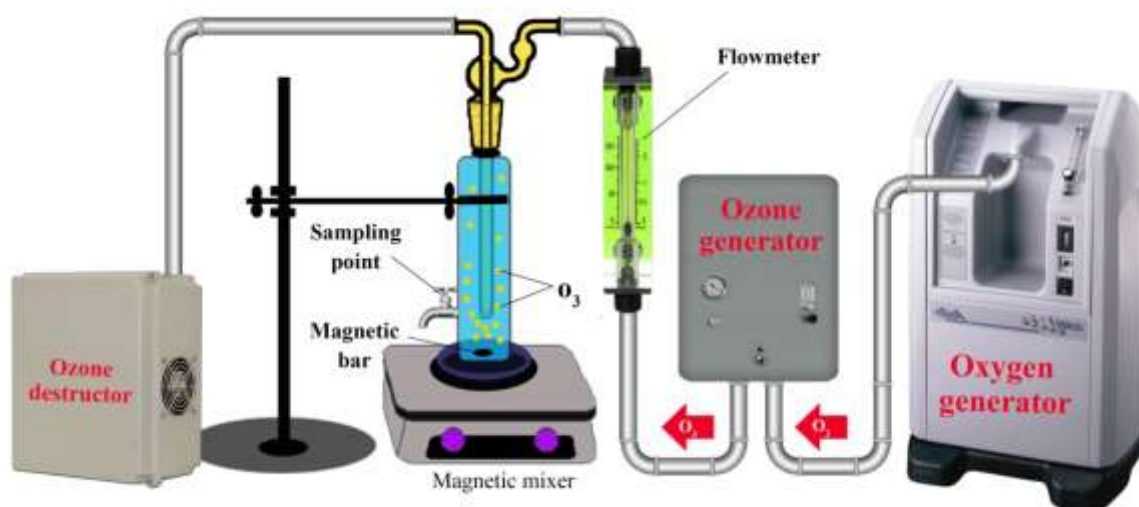


Fig. 3. Schematic of experimental set-up of catalytic ozonation system.

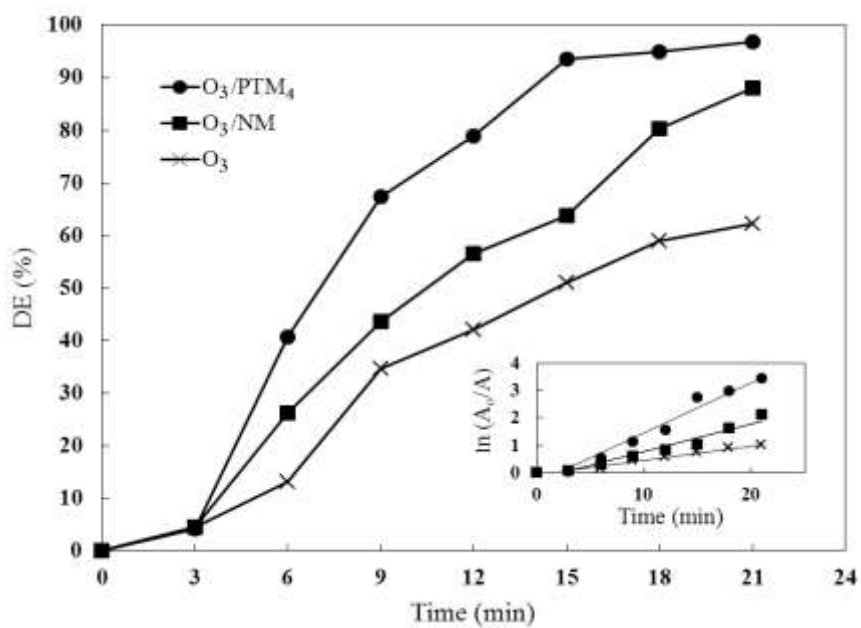


Fig. 4. Comparison of O₃, O₃/NM and O₃/PTM₄ ozonation in degradation of BB3. The inset shows mentioned processes follow pseudo-first order kinetic. Experimental conditions: catalyst dose: 600 mg/L, initial BB3 concentration: 90 mg/L, ozone concentration: 1.2 g/L and initial pH: 6.7.

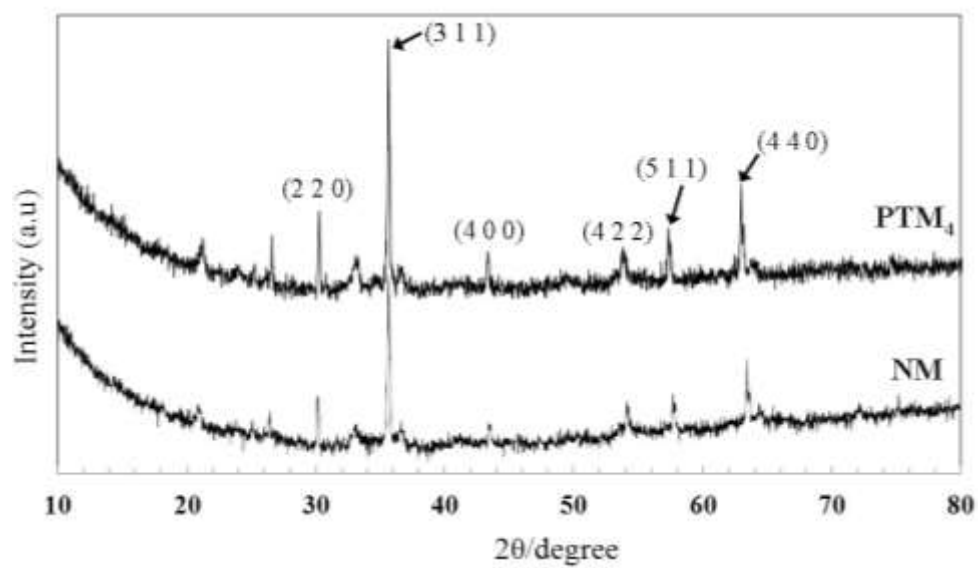


Fig. 5. XRD patterns of NM and PTM₄ samples.

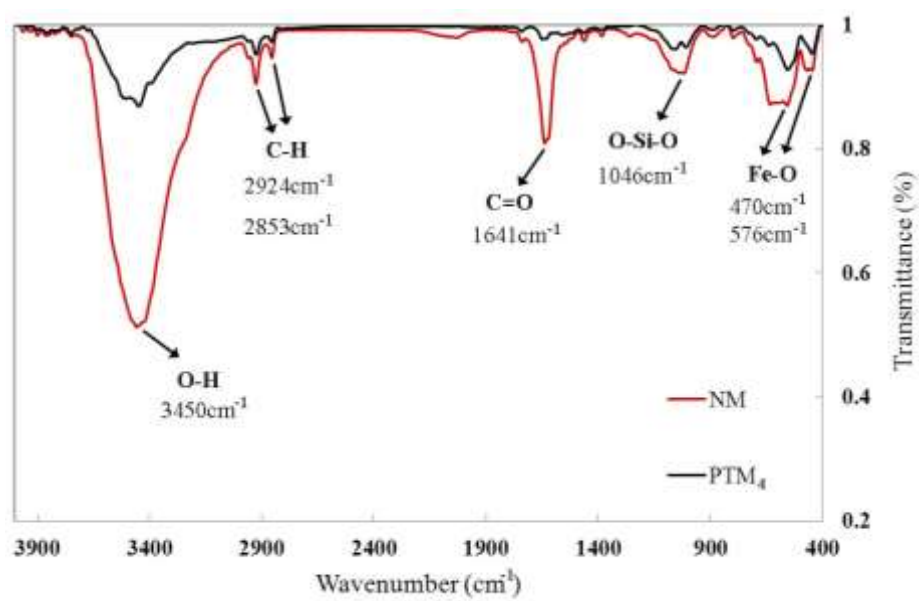


Fig. 6. FT-IR spectra of NM and PTM₄ samples.

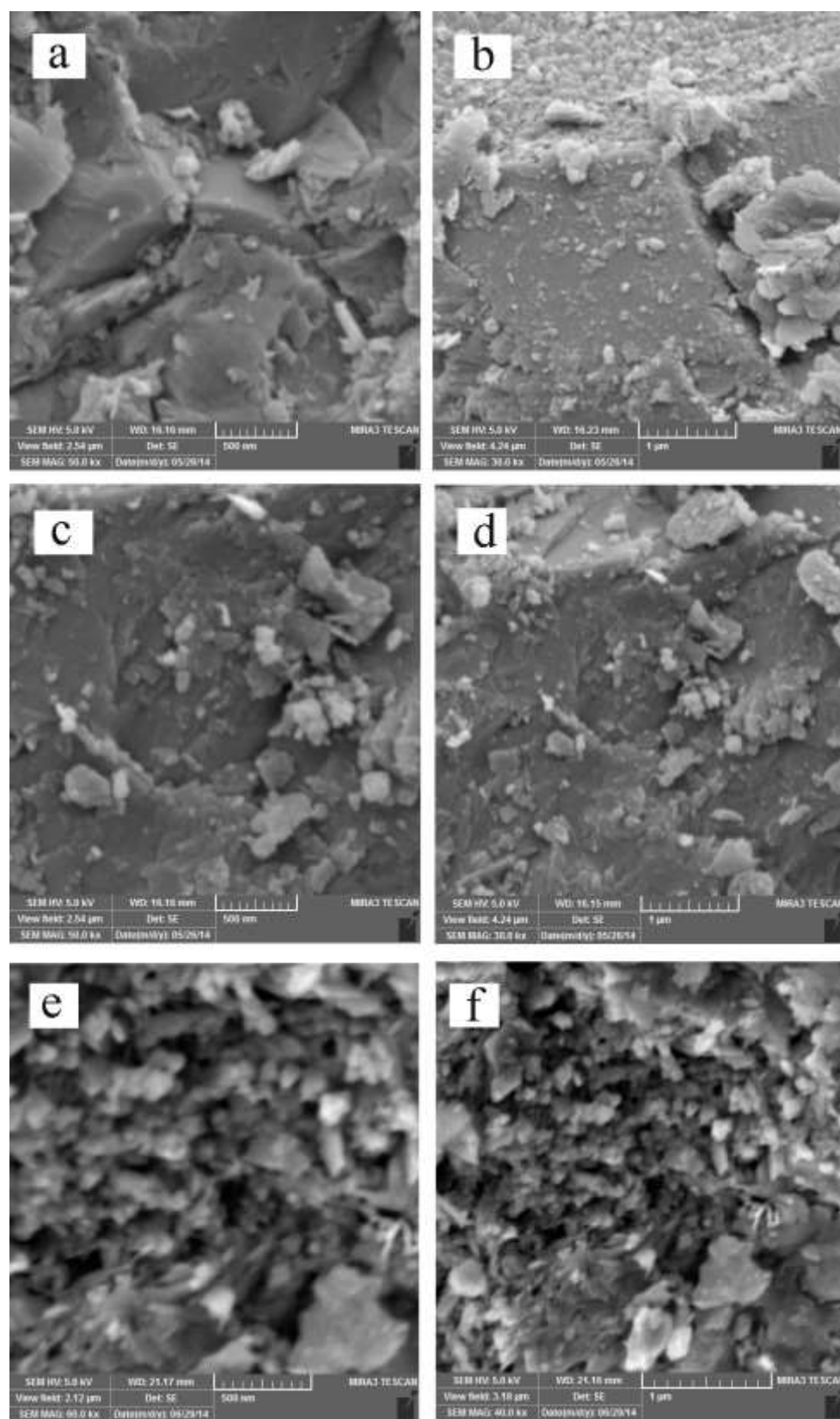


Fig. 7. SEM images of NM (a, b), NM exposure to O₂ plasma (15 min) (c, d) and PTM₄ (e, f).

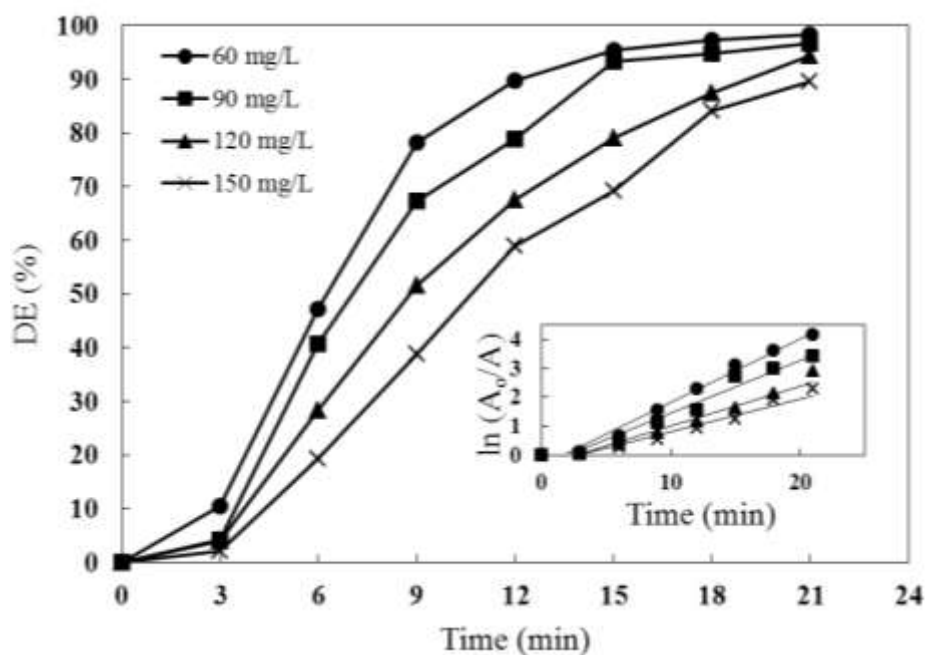


Fig. 8. Effect of initial BB3 concentration on the degradation of BB3 during PTM4 catalytic ozonation. The inset shows mentioned processes follow pseudo-first order kinetic. Experimental conditions: PTM₄ dose: 600 mg/L, ozone concentration: 0.3 g/L and initial pH: 6.7.

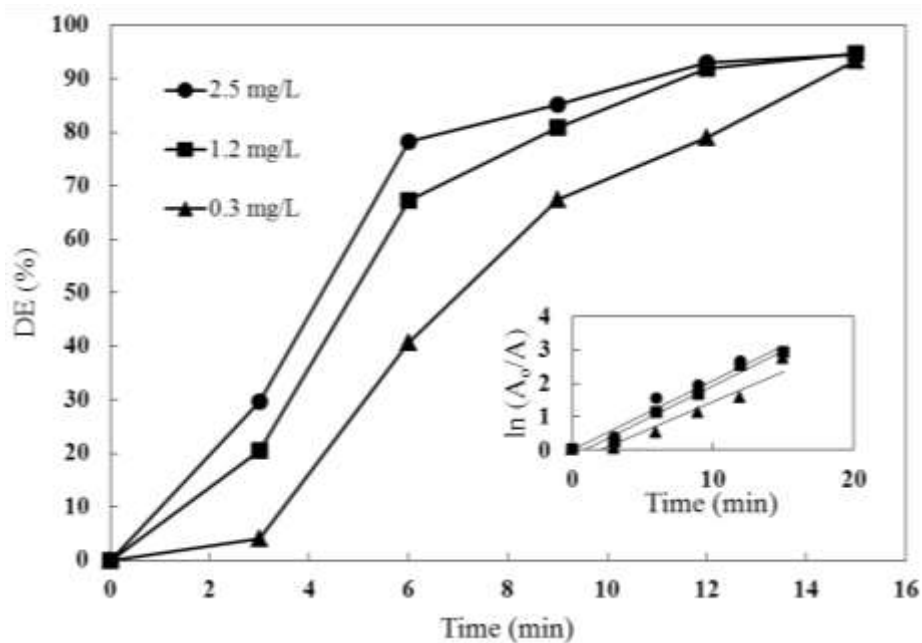


Fig. 9. Effect of ozone concentration on the degradation of BB3 during PTM₄ catalytic ozonation. The inset shows mentioned processes follow pseudo-first order kinetic. Experimental conditions: PTM dose: 600 mg/L, initial BB3 concentration: 90 mg/L and initial pH: 6.7.

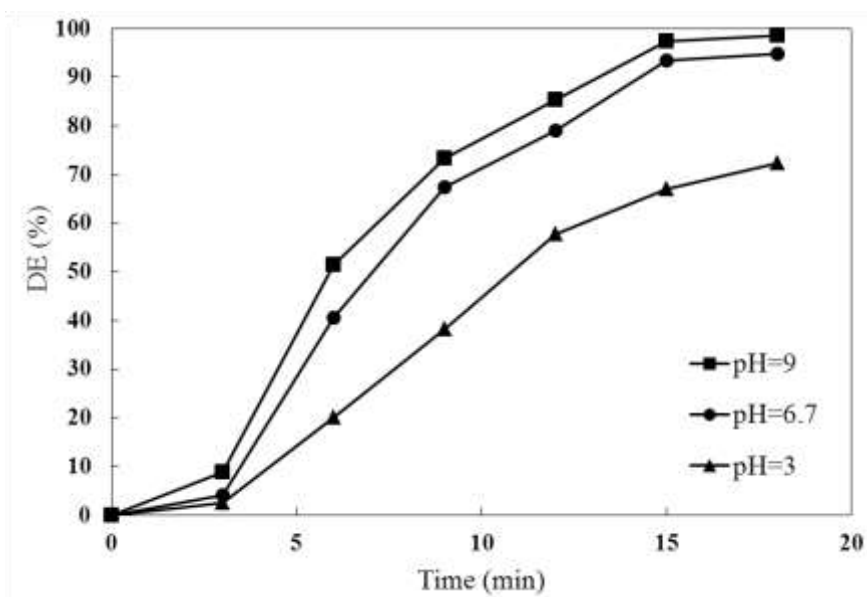


Fig. 10. Effect of initial pH on the PTM₄ catalytic ozonation of BB3. Experimental conditions: PTM dose: 600 mg/L, initial BB3 concentration: 90 mg/L and ozone concentration: 0.3 g/L.

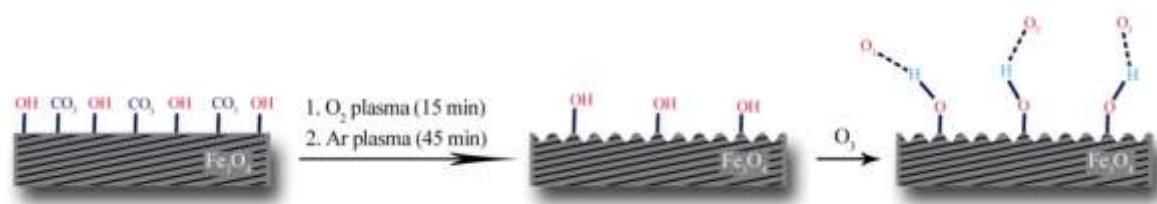


Fig. 11. Proposed model for the interaction of glow discharge (O_2 -Ar) plasma and O_3 with catalyst surface.

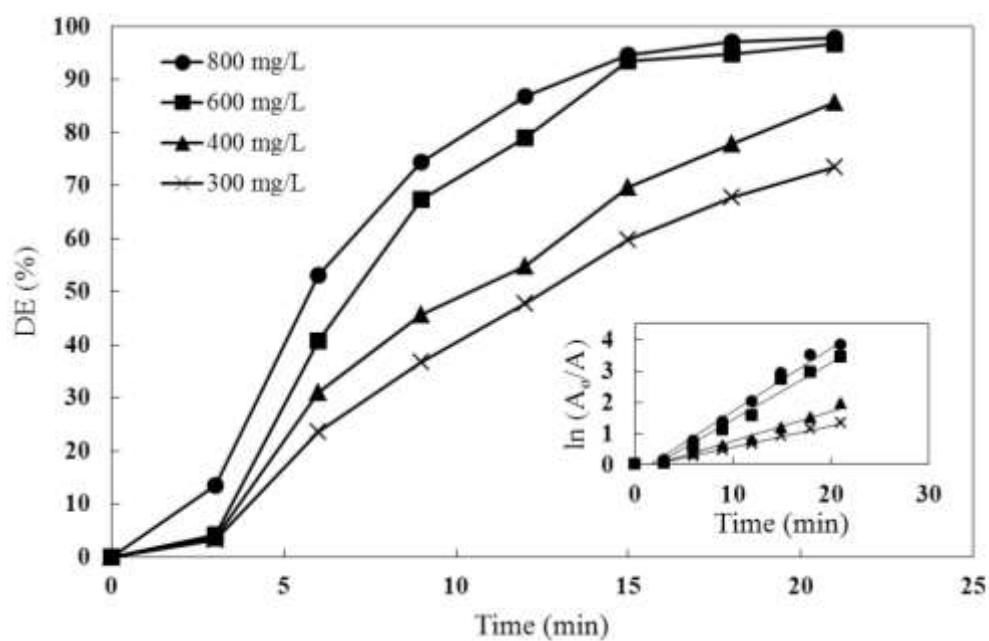


Fig. 12. Effect of initial PTM₄ concentration on the catalytic ozonation of BB3. The inset shows mentioned processes follow pseudo-first order kinetics. Experimental conditions: initial BB3 concentration: 90 mg/L, ozone concentration: 0.3 g/L and initial pH: 6.7.

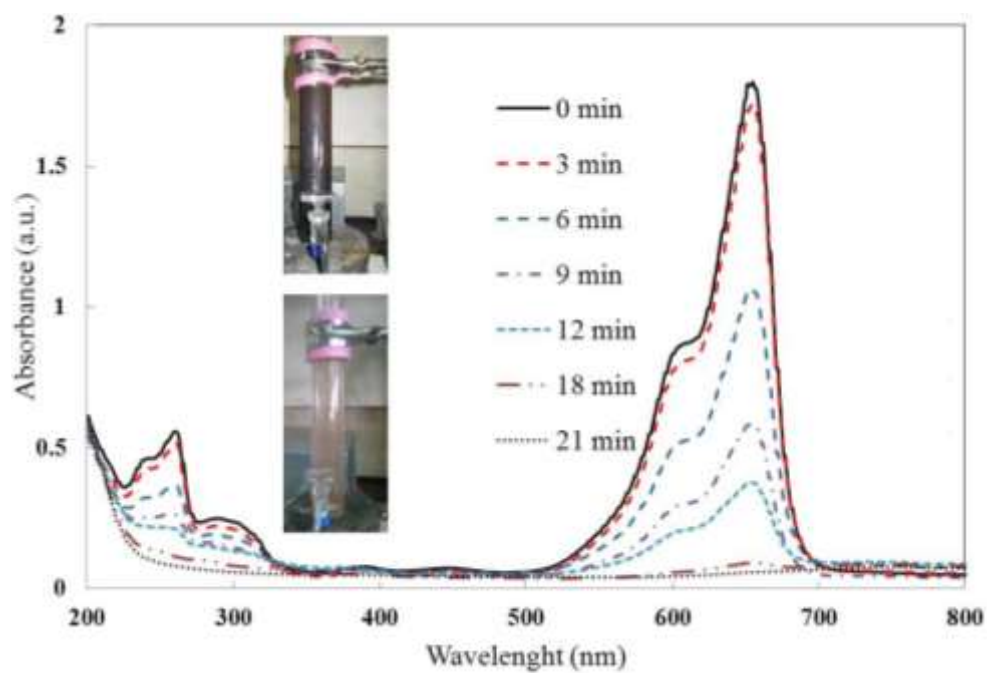


Fig. 13. Change in UV-Visible spectra of BB3 solution PTM₄ catalytic ozonation process at different times. Experimental conditions: catalyst dose: 600 mg/L, initial BB3 concentration: 90 mg/L, ozone concentration: 0.3 g/L and initial pH: 6.7.

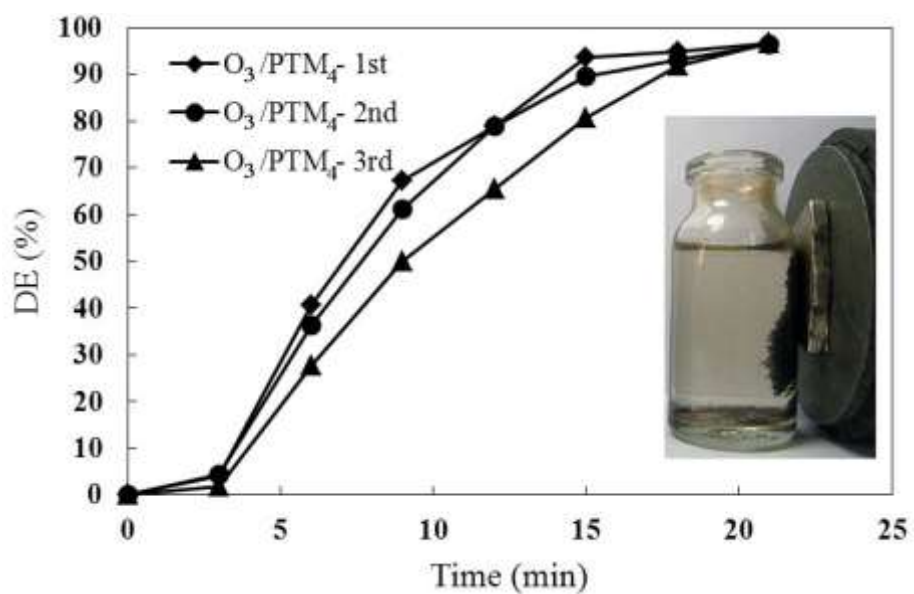


Fig. 14. Reusability of PTM₄ on PTM₄ catalytic ozonation of BB3. Experimental conditions: PTM dose: 600 mg/L, initial BB3 concentration: 90 mg/L, ozone concentration: 0.3 g/L, and initial pH: 6.7.

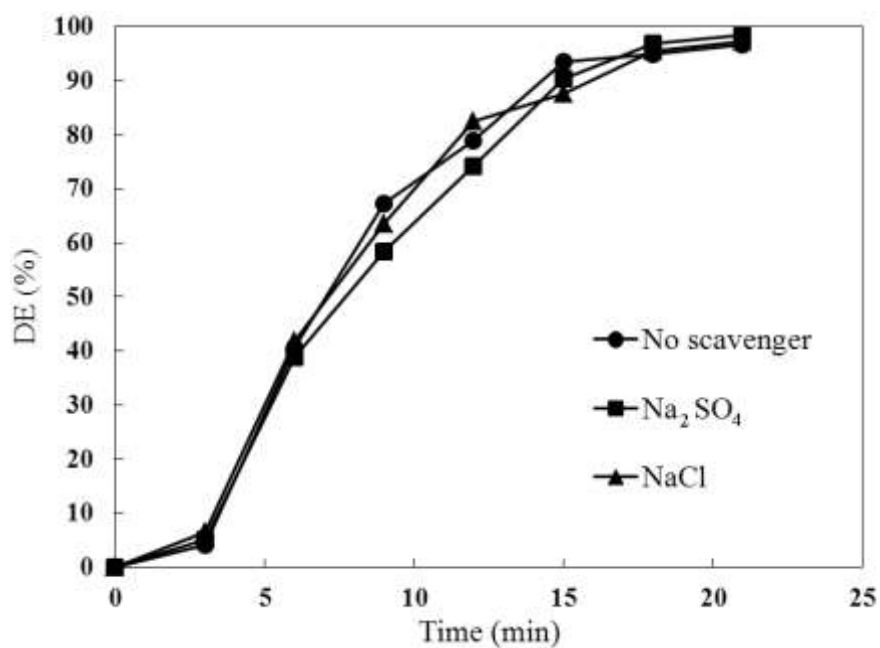


Fig. 15. Effect of addition different salts on the degradation of BB3 during PTM₄ catalytic ozonation. Experimental conditions: PTM₄ dose: 600 mg/L, initial BB3 concentration: 90 mg/L, initial salts concentration: 1 mM, ozone concentration: 0.3 g/L, and initial pH: 6.7.

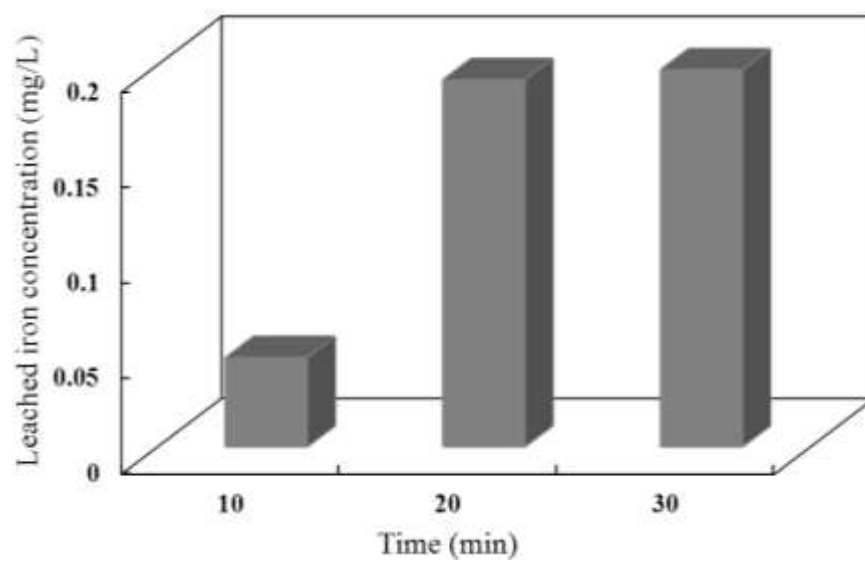


Fig. 16. Evolution of total iron leached from the PTM₄ catalyst. Experimental conditions: PTM dose: 600 mg/L, ozone concentration: 0.3 g/L and initial pH: 6.7.